CHEMISTRY OF MATERIALS
Article

Chem. Mater. **2010,** *22,* 5445–5452 5445
DOI:10.1021/cm100729d

High-κ Dielectric Sol−Gel Hybrid Materials Containing Barium Titanate Nanoparticles

Jina Chon, Saemi Ye, Kyoung Jin Cha, Seong Chul Lee, Yong Sung Koo, Jong Hoon Jung,* and Yong Ku Kwon*

Department of Polymer Science and Engineering and Department of Physics, Inha University, Incheon 402-751, Korea

Received March 12, 2010. Revised Manuscript Received August 20, 2010

Novel high-κ thin composite films with excellent breakdown strength were synthesized using nonhydrolytic sol−gel processing. Organic−inorganic hybrid materials with high electronic polarizability were prepared as the matrix material to form a covalently bonded interface with the organically modified barium titanate (TBT) nanoparticles through a chemical cross-linking reaction. To enhance the dispersion stability of barium titanate (BT) nanoparticles in the matrix, the chemical nature of their surfaces was modified using diethyl 3-(trimethoxysilyl)propyl phosphonate (TMSP), which was synthesized by the Michaelis−Arbuzov reaction of chloropropyltrimethoxysilane (CPTMS) with 3-triethyl phosphate (TEP). A high degree of dispersion of the dielectric BT nanoparticles significantly improved the dielectric properties of the final composite films. Because the matrix consists of both silane and halogenated bisphenol A moieties with high electronic polarizability, adjusting the chemical composition allowed tailoring of the dielectric and film properties of the final composite materials.

Introduction

High-performance dielectric materials, known as high-κ materials, are expected to play increasingly important roles in the next generation of electronics and very large scale integrated (VLSI) microelectronics technology.[1−10] Silica-based ceramic materials, such as silica (SiO_2),[1] hafnium silicate ($HfSiO_4$),[8] and zirconium silicate ($ZrSiO_4$),[8] are common interlayer dielectric materials used in high density microelectronic packaging. Barium titanate ($BaTiO_3$, denoted as BT)[7] is one of well-known dielectric materials that is also used in a variety of semiconductor devices owing to its high and frequency-independent permittivity with low dielectric loss.[7,11−13] These inorganic compounds have the disadvantages of limited tunability of their own dielectric properties, high production cost and poor processability. Polymeric materials have been also been used in the electronic packaging industry on account of their versatility, flexibility, lightweight, low cost, and ease of modification with high dielectric strength. However, regardless of the chemical nature of the polymer backbones and alternating current frequency, most of these covalently bonded polymers have relatively low dielectric constants (< 9), which limits their extensive use in the microelectronic packaging and passive semiconductor industry.[14]

Recently, a variety of polymer composite materials, in which two or more different phases with complementary physical properties were combined, were developed to achieve material properties superior to those of single organic or inorganic components.[15−18] Their advantages of flexibility, lightweight, low cost, and ease of processing, as well as tunable properties, make them potentially applicable in a variety of fields. Moreover, their dielectric properties can also be tuned by changing the composition

*Corresponding author. Tel: +82-32-860-7482. Fax: +82-32-865-5178. E-mail: jhjung@inha.ac.kr (J.H.J.); ykkwon@inha.ac.kr (Y.K.K.).

(1) Wilk, G. D.; Wallace, R. M.; Anthony, J. M. *J. Appl. Phys.* **2001**, *89*, 5243–5275.
(2) Chen, F.; Chu, C.; He, J.; Yang, Y.; Lin, J. *Appl. Phys. Lett.* **2004**, *85*, 3295–3297.
(3) Windlass, H.; Raj, P.; Balaraman, D.; Bhattacharya, S.; Tummala, R. *IEEE Trans. Electron. Packag. Manuf.* **2003**, *26*, 100–105.
(4) Rao, Y.; Ogitani, S.; Kohl, P.; Wong, C. P. *J. Appl. Polym. Sci.* **2002**, *83*, 1084–1090.
(5) Huang, C.; Zhang, Q. M.; Su, J. *Appl. Phys. Lett.* **2003**, *82*, 3502–3504.
(6) Zhang, Q. M.; Li, H.; Poh, M.; Cheng, Z.; Xu, H.; Xia, F.; Huang, C. *Nature* **2002**, *419*, 284–287.
(7) Arlt, G.; Hennings, D.; De With, G. *J. Appl. Phys.* **1985**, *58*, 1619–1625.
(8) Wilk, G. D.; Wallace, R. M.; Anthony, J. M. *J. Appl. Phys.* **2000**, *87*, 484–492.
(9) Lee, B. H.; Kang, L.; Nieh, R.; Qi, W. J.; Lee, J. C. *Appl. Phys. Lett.* **2000**, *76*, 1926–1928.
(10) Copel, M.; Gribelyuk, M.; Gusev, E. *Appl. Phys. Lett.* **2000**, *76*, 436–438.
(11) MacChesney, J .B.; Gallagher, P. K.; di Marcello, F. V. *J. Am. Ceram. Soc.* **1963**, *46*, 197–202.
(12) Shi, Z. Q.; Jia, Q. X.; Anderson, W. A. *J. Electron. Mater.* **1991**, *20*, 939–944.
(13) Shi, Z. Q.; Jia, Q. X.; Anderson, W. A. *J. Vac. Sci. Technol., A* **1993**, *11*, 1411–1413.
(14) Cha, H. J.; Hedrick, J.; DiPietro, R. A.; Blume, T.; Beyers, R.; Yoon, D. Y. *Appl. Phys. Lett.* **1996**, *68*, 1930–1932.
(15) Kim, P.; Jones, S. C.; Hotchkiss, P. J.; Haddock, J. N.; Kippelen, B.; Marder, S. R.; Perry, J. W. *Adv. Mater.* **2007**, *19*, 1001–1005.
(16) Xu, J.; Wong, C. P. *Appl. Phys. Lett.* **2005**, *87*, 082907/1–082907/3.
(17) Xu, J.; Wong, C. P. *J. Electron. Mater.* **2006**, *35*, 1087–1094.
(18) Dang, Z.-M.; Lin, Y.-Q.; Xu, H.-P.; Shi, C.-Y.; Li, S.-T.; Bai, J. *Adv. Funct. Mater.* **2008**, *18*, 1509–1517. Dang, Z.-M.; Zhou, T; Yao, S.-H.; Yuan, J.-K.; Zha, J.-W.; Song, H.-T.; Li, J.-Y.; Chen, Q.; Yang, W.-T.; Bai, J. *Adv. Mater.* **2009**, *21*, 2077–2082.

Published on Web 09/16/2010

of the fillers or chemical nature of the polymeric materials. The polymers used to produce high-κ composite materials, include polyimide,[15,18] polycarbonate,[15] and thermosetting resins,[17,19] which are relatively easy to fabricate and can be processed into thin films by wet processing. BT, $Pb(ZrTi)O_3$, and $PbTiO_3$ have been used as inorganic fillers for dielectric applications.[20] Although these composite materials have many advantages, such as tunable dielectric behavior, easy fabrication and low production cost, they experience significant dielectric loss, particularly at the moderate to high ceramic loadings needed to achieve the optimum dielectric performance in semiconductor devices.

As part of an ongoing search for new materials suitable for interlayer dielectrics in thin film packaging, this study synthesized a novel high-κ thin composite film with extremely high breakdown strength. To this end, organic−inorganic hybrid materials with high electronic polarizability were prepared as the matrix material to form a covalently bonded interface with the organically modified BT nanoparticles through a chemical cross-linking reaction. The main reason for using this hybrid matrix is to achieve a high degree of dispersion of the dielectric BT nanoparticles, which significantly improves the dielectric properties of the final composite films. Since the matrix consists of both silane and halogenated bisphenol A moieties with high electronic polarizability, adjusting the chemical composition may allow tailoring of the dielectric properties of the final composite materials. Another advantage is the excellent mechanical integrity, as evidenced by its flexibility, toughness, and adhesion, which can be tailored to meet the needs of specific electronic applications. A facile nonhydrolytic sol−gel processing method can be used to produce crack-free composite films with no remaining traces of solvents.[21−27] This method avoids the high volume shrinkage during further treatment of the films, making it suitable for soft molding processes.

Experimental Section

Materials. Triethyl phosphite (TEP, 98%), 3-(trimethoxysilyl)-propylmethacrylate (ATMS, 98%), 4,4′-(hexafluoroisopropyldene)-diphenol (FBPA, 97%), barium hydroxide monohydrate (98%), and 2,2′-dimethoxy-2-phenyl-acetophenone (DPA, 99%) were purchased from Aldrich. BT nanoparticles with a mean diameter of 50−80 nm were obtained from Alfa Aesar. 3-Chloropropyltrimethoxysilane (CPTMS, 98% was supplied by JSI silicone, and polydimethylsiloxane (PDMS, Sylgard 184) was acquired from Dow Corning. All chemicals and solvents were used without further purification.

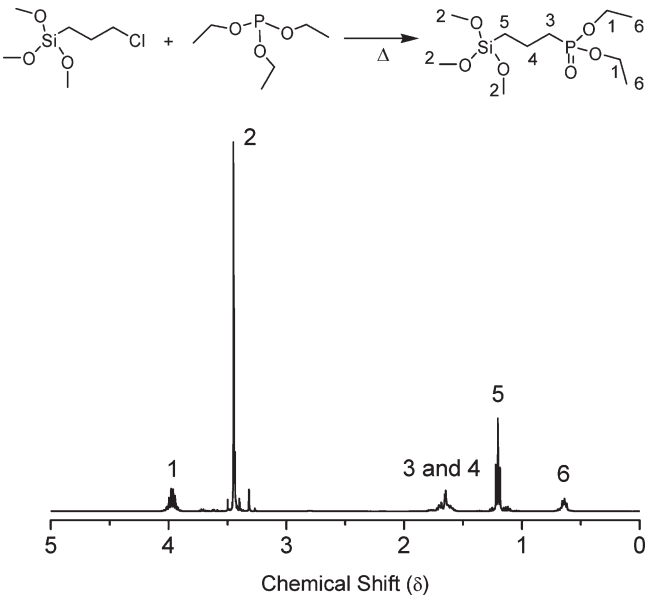

Figure 1. ^{1}H NMR spectra of diethyl 3-(trimethoxysilyl)propyl phosphonate (TMSP).

Characterization. The ^{1}H spectra were recorded on a Varian Unityinova 400 spectrometer at 400 MHz and were referenced to tetramethylsilane (TMS). FTIR spectra were obtained with a Nicolet, Magna 7509 spectrometer. Fibrous sample were reduced to small pieces before mixing with potassium bromide, by cutting with scissors to very short length and rolling in a mill to film-like geometry. Transmission electron microscopy (TEM) and scanning electron microscopy (SEM) measurements of the BT and TBT nanoparticles were conducted on a Phillips CM-220 and Hitachi S-4200, respectively. The complex dielectric constant of the composite films was measured at frequencies (Hz) of 1×10^3 to 1×10^6 with excitation of 1 V using an LCR meter. A series of thin films of composite materials were prepared by spin-coating viscous solutions onto an ITO substrate, followed by photocuring under UV irradiation (λ = 365 nm). Parallel plate type capacitors of the composite films were then prepared by evaporating the Ag electrodes on the top of the thin composite film. Dielectric breakdown strength was measured by a Keithley 236 Source Measurement Unit by sweeping the applied voltage up to 15 V and estimated by the specific voltage at which a sharp increase of current occurs. Electrodes for breakdown strength are the same as those used for dielectric constant measurement. In detail, the composite was deposited on a In_2O_3:Sn (ITO)-coated glass and the Ag was evaporated on the top of the composite with area of 4 mm^2. After the Cu wires were attached on both Ag and ITO electrodes, the heat treatment at 150 °C for 5 min was performed for good adhesion. The average thickness of the spin-coated films was approximately 3 μm, and the volume fraction of the nanoparticles in the mixture was 14%.

Synthesis of Diethyl 3-(trimethoxysilyl)propyl Phosphonate (TMSP). TMSP was successfully synthesized by Michaelis-Arbuzov reaction of chloropropyltrimethoxy-silane (CTMS) and 3-triethyl phosphate (TEP). ^{1}H NMR ($CDCl_3$, ppm): δ 3.95 (q, 4H, $-O-CH_2CH_3$), 3.43 (s, 9H, $-OCH_3$), 1.63−1.69 (m, 4H, $-PCH_2CH_2-$ and $-PCH_2CH_2-$), 1.20 (t, 6H, $-O-CH_2CH_3$), 0.63 (t, 2H, $-Si-CH_2CH_2-$).

(19) Cho, S.-D.; Lee, S.-Y.; Hyun, J.-G.; Paik, K.-W. *J. Mater. Sci. Mater. Electron.* **2000**, *11*, 253–268.
(20) Dąbrowski, J.; Lippert, G.; Oberbeck, L.; Schröder, U.; Costina, I.; Lupina, G.; Ratzke, M.; Zaumseil, P.; Müssiga, H.-J. *J. Electrochem. Soc.* **2008**, *155*, G97–G114.
(21) Lowry, J. H.; Mendlowitz, J. S.; Subramanian, N. S. *Opt. Eng.* **1992**, *31*, 1982–1985.
(22) Hale, D. K. *J. Mater. Sci.* **1976**, *11*, 2105–2141.
(23) Saegusa, T.; Chujo, Y. *Makromol. Chem. Macromol. Symp.* **1992**, *64*, 1–9.
(24) Novak, B. M. *Adv. Mater.* **1993**, *5*, 422–433.
(25) Sanchez, C.; Ribot, F. *New J. Chem.* **1994**, *18*, 1007–1047.
(26) Brinker, C. J.; Scherer, G. W. *Sol−Gel Science*; Academic Press: Boston, 1990.
(27) Kwon, Y. K.; Han, J. K.; Lee, J. M.; Ko, Y. S.; Oh, J. H.; Lee, H.-S.; Lee, E.-H. *J. Mater. Chem.* **2008**, *18*, 579–585.

Scheme 1

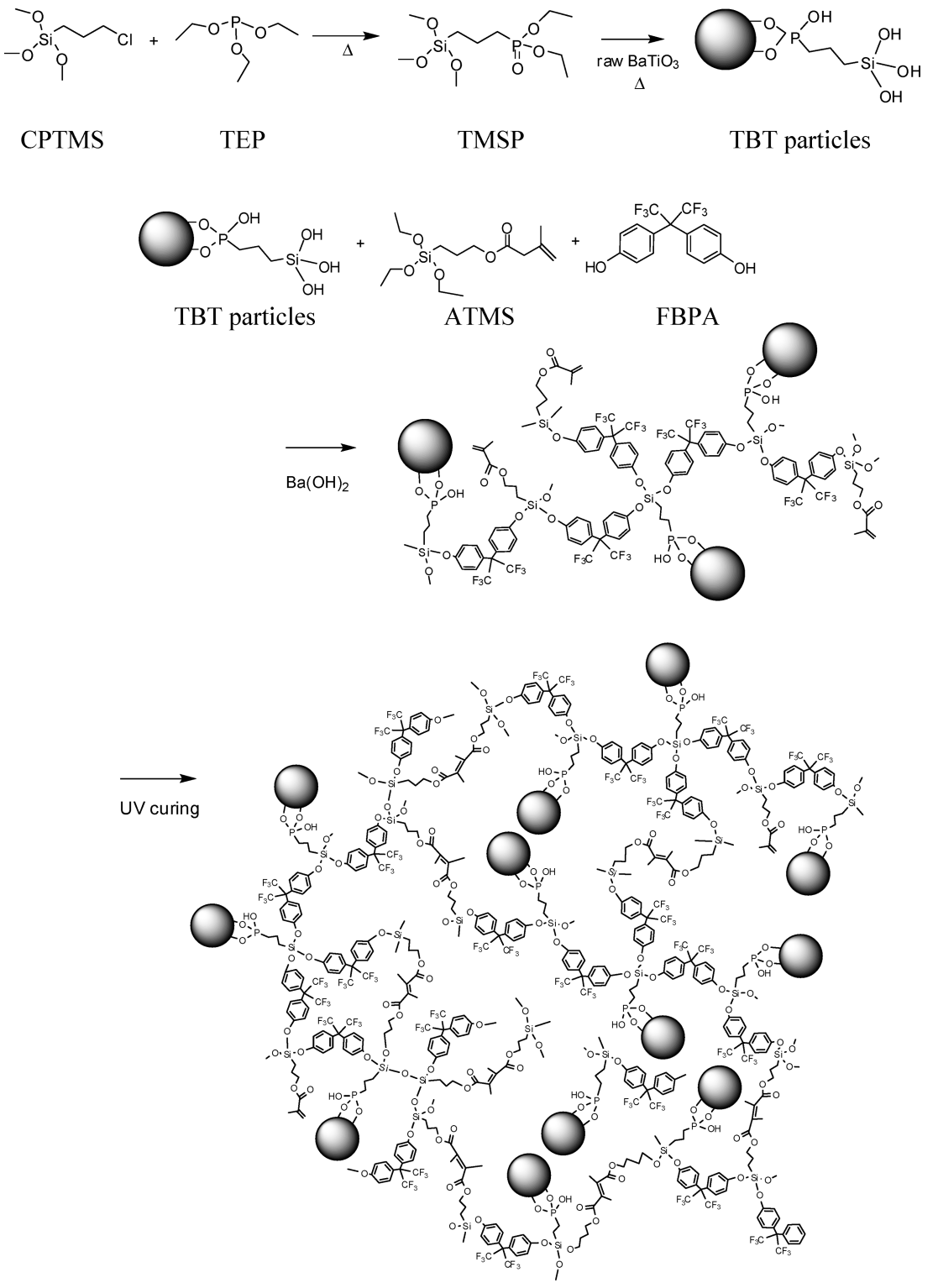

Results and Discussion

Surface Modification of BT Nanoparticles. The dispersion stability and aggregation behavior of ceramic nanoparticles in polymer matrices are some of the key variables for determining the dielectric and film properties of ceramic/polymer composites. It was reported that the dielectric constant of polymer composite films containing nanometer-sized BT particles increases with increasing volume fraction of BT particles.[28] However, most polymer composite films with high BT loadings often contain aggregates of BT particles, which cause voids or cavities near the interfaces with the matrix that reduces the breakdown strength and dielectric performance of the final composite films in many practical uses. To enhance the

(28) Kobayashi, Y.; Tanase, T.; Tabata, T.; Miwa, T.; Konno, M. *J. Eur. Ceram. Soc.* **2008**, *28*, 117–122.

dispersion stability of the BT nanoparticles in the matrix, we modified the chemical nature of their surfaces using TMSP, which was synthesized by the Michaelis−Arbuzov reaction[29,30] of CPTMS with TEP. In this reaction, 120 mL of TEP was heated to 130 °C with stirring followed by the slow addition of 60 mL of CTMS over 90 min while heating to 150−160 °C. The mixture of CTMS and TEP was stirred continuously for an additional 12 h under reflux and then cooled to room temperature. Excess TEP and other possible impurities were removed under reduced pressure through a short path distillation apparatus. The crude product was purified by vacuum distillation at 120 °C. The chemical structure of the final product TMSP was confirmed by ^{1}H NMR, as shown in Figure 1. Scheme 1 gives a schematic diagram of the synthetic pathway of TMSP.

For the surface modification of the BT nanoparticles, the BT nanoparticles were initially dispersed in a 95:5 (v/v) ethanol/H_2O mixture, followed by the addition of 0.2 g of TMSP. TMSP was added to 10 mL of a 95:5 (v/v) ethanol/H_2O mixture containing 0.4 g of the raw BT nanoparticles to obtain the TMSP-coated BT nanoparticles (TBT). The mixture of BT and TMSP was ultrasonicated for 10 min and stirred at 80 °C for an additional 1 h. These TBT nanoparticles were separated by centrifugation and rinsed 3 times with excess absolute ethanol with ultrasonication at room temperature followed by centrifugation. After washing, the TBT nanoparticles were freeze-dried. It was reported that most of the phosphonate compounds as a surface modifier is bound to the surface of BT nanoparticles in a tridentate form, as shown in Scheme 1. The successful grafting of TMSP on the surfaces of the BT nanoparticles was confirmed by TEM and EDS, as shown in Figure 2.

As described earlier, the chemical modification of BT nanoparticles can lead to a high degree of dispersion in the hybrid matrix. The strong binding ability of TMSP onto the surfaces of the BT nanoparticles can be provided by its phosphonate unit at one end. The trimethoxysilane moiety of TMSP provides the affinity with the hybrid matrix sol and the ability for the reaction with the silane-based hybrid matrix to achieve a high degree of dispersion without voids or cavities both within the matrix and in the interfacial region between the organically modified BT nanoparticles and hybrid matrix. BT particles with average diameters of 50−80 nm and 4 μm are denoted as BT65 and BT400, respectively, and were used for the grafting reaction with TMSP. The corresponding organically modified BT65 and BT400 particles prepared by a reaction with TMSP are denoted as TBT65 and TBT400, respectively.

The successful grafting of TMSP onto the surfaces of the BT nanoparticles was confirmed by transmission electron microscopy (TEM) and energy dispersive spectroscopy (EDS). Figure 2a shows TEM images of TBT65.

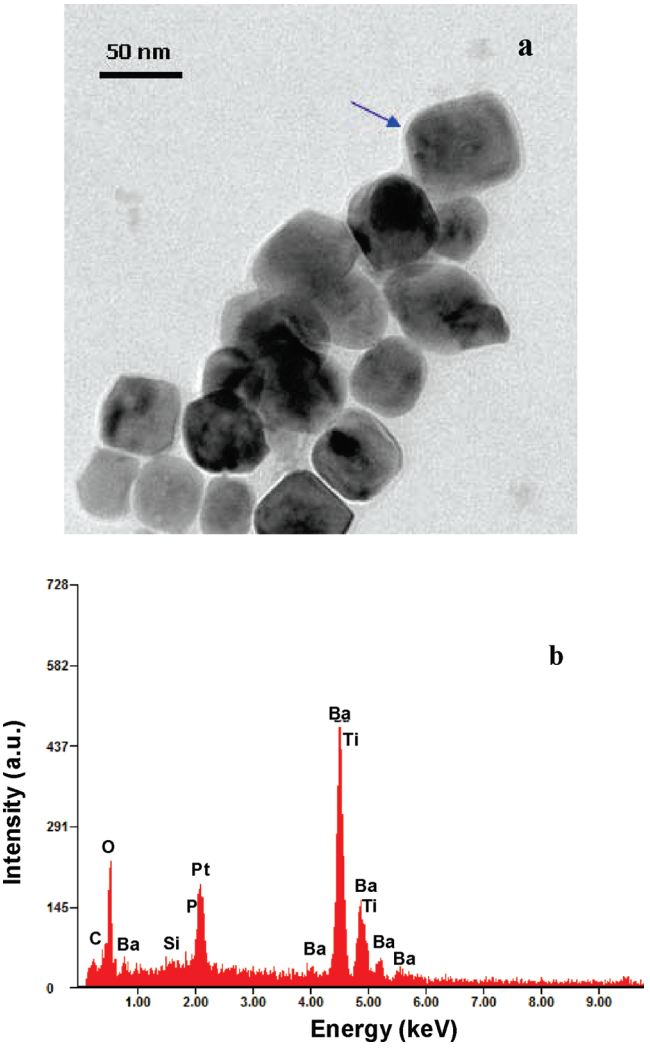

Figure 2. (a) Transmission electron microscopy (TEM) image of the TBT nanoparticles with average diameters of 50−80 nm and (b) their energy dispersive spectroscopy (EDS) data.

In this figure, the nanoparticles were coated uniformly with the organic layer of TMSP, confirming the successful grafting of the organic layer onto the BT nanoparticles. The EDS data of the TBT65 nanoparticles, as shown in Figure 2b, clearly shows Si, P, and C peaks due to the organic layer, also indicating the formation of the organic layer on the BT nanoparticles.

High-κ Composite Films. To prepare the composite material with TBT nanoparticles by sol−gel processing, 3 g of ATMS and 0.1 mol % of the total silane compound of $Ba(OH)_2 \cdot H_2O$ were mixed at 80 °C under dry N_2 conditions. $Ba(OH)_2 \cdot H_2O$ was added as a catalyst to promote a condensation reaction between two components. TBT65 or TBT400, as the inorganic fillers, was then added to the mixed sol of ATMS and $Ba(OH)_2 \cdot H_2O$. The organic diol of 4,4′-(hexafluoroisopropyldene)diphenol (FBPA, 97%) was then added continuously to mixtures of the ATMS/$Ba(OH)_2 \cdot H_2O$ containing the TBT particles, and stirred for 30 min to form the silica-type networks based on Si−O−Si bonds through the nonhydrolytic sol−gel reaction. The amount of the FBPA diol was fixed to 30 mol % ATMS, while that of catalyst was fixed to 0.1 mol % of

(29) Bhattacharya, A. K.; Thyagarajan, G. *Chem. Rev.* **1981**, *81*, 415–430.
(30) Guerrero, G.; Mutin, P. H.; Vioux, A. *Chem. Mater.* **2000**, *12*, 1268–1272. Lee, B. I. *J. Electroceram.* **1999**, *3*, 53–63.

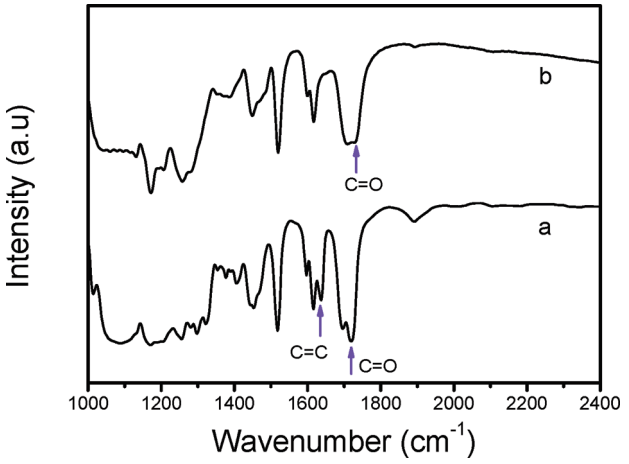

Figure 3. FTIR absorption spectra of (a) the as-prepared hybrid gel and (b) the cured film after being exposed by UV light for 5 min.

the total amount of the silane compound. The mixed sol was kept at 80 °C for an additional 4 h to allow the reaction to proceed under sonication. After the reaction, the resulting solution was kept at 100 °C for 2 h in a vacuum oven to remove the methanol and other impurities, and then cooled to room temperature.

The photopolymerization of the unreacted C═C bonds of ATMS was performed using 2,2-dimethoxy-2-phenylacetophenone as a UV initiator. The concentration of the photoinitiator was 2 mol % of the total C═C bonds in ATMS and the volume fraction of the TBT nanoparticles of 14% was used to maintain the flexibility of the final composite films. Thin films of the final, viscous composite solutions were obtained by spin coating onto a glass substrate at rotation speeds between 800 and 1500 rpm. The spin-coated films were exposed to UV light for cross-linking at room temperature. The cured films, covered by poly(dimethyl siloxane) film were heat-treated for 30 min at 70 °C for postcuring. FBPA was reacted with ATMS to form inorganic silica-type networks based on the Si−O−Si bonds in the sol−gel reaction.

FTIR absorption spectroscopy data, demonstrated in Figure 3 was performed on the as-prepared hybrid gel (curve *a*) and cured film after exposure to UV light for 5 min (curve *b*). The peak at 1638 cm^{-1}, which was assigned to the C═C bond of the ATMS precursor, had disappeared in the cured film. This indicates that the C═C bonds of ATMS had transformed completely into the C−C bonds during photopolymerization. The peak for the C═O band (1720−1740 cm^{-1}) was also shifted to a higher wavenumber due to the absence of conjugation with the C═C bond after photopolymerization. The change observed in the FTIR absorption spectra was attributed to the complete transformation of the C═C bonds of the methacrylate groups to C−C bonds during UV-induced photopolymerization. These films were thermally stable up to almost 400 °C and exhibited less than 10% weight loss when heated to 400 °C. The slight weight loss near 100 °C was due mainly to the evaporation of the remaining methanol or water on the samples during the heating process. These films were removed easily from the ITO substrate without any deformation, and they showed excellent toughness and strength when subjected to elongation testing.

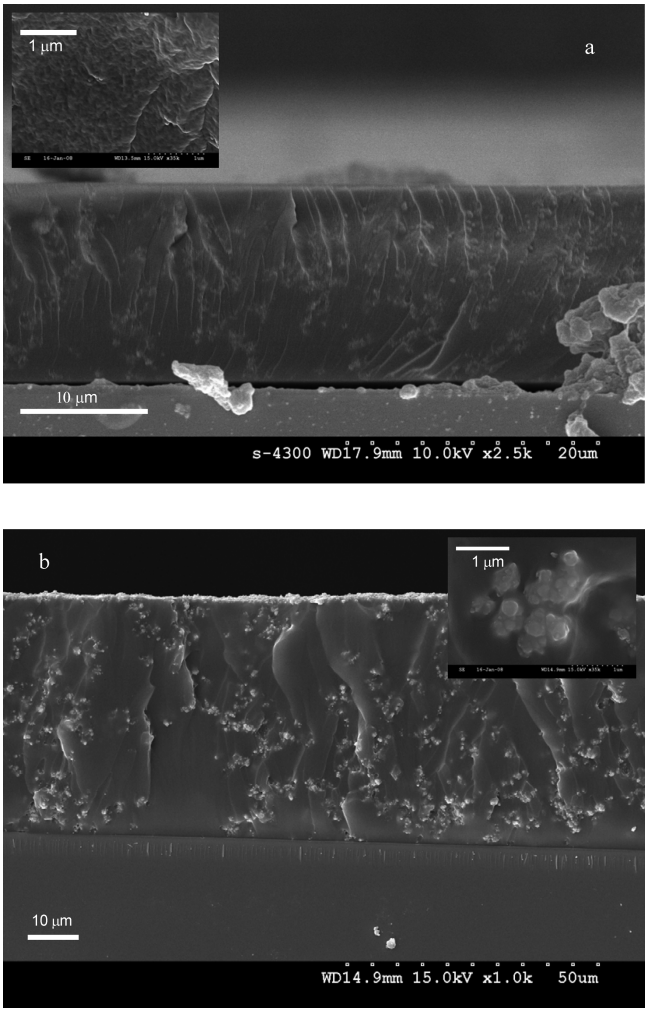

Figure 4. Scanning electron microscopy (SEM) images of cross-sections of the as-cast films of organic−inorganic hybrids with the (a) TBT65 and the (b) BT65 nanoparticles.

Images a and b in Figure 4 show SEM images of a cross-section of the spin-coated films containing TBT65 and BT65 nanoparticles, respectively. In Figure 4a, the composite film exhibited excellent wetting with the ITO substrate, and their film-to-air surfaces were flat and smooth without voids, indicating excellent peel strength and solder resistance suitable for printed wiring applications. In this image, the TBT65 particles were covered completely by the hybrid matrix, displaying excellent interfacial adhesion of the TBT particles to the hybrid matrix. This excellent interfacial quality was obtained by a sol−gel reaction between the trimethoxysilane units of TMSP, which were located on the TBT nanoparticles and the silane moieties of the hybrid matrix of ATMS and FBPA at their interfaces. In addition, the hydroxyl units, possibly located on the TBT nanoparticles have strong affinity with the hybrid matrix, containing both siliane and hydroxyl moieties. In Figure 4b, the composite films with the unmodified BT nanoparticles, which were prepared under the same conditions as those used in

Figure 4a, exhibited a rough and nonuniform film surface along with aggregates of BT particles within the matrix. This suggests that grafting of TMSP on the BT nanoparticles is essential for achieving smoother, defect-free thin films with a high degree of dispersion and interfacial quality of the BT nanoparticles in the hybrid matrix. The thickness of the spin-coated layer could be adjusted from the nanometer to micrometer scale simply by changing the composition of the ATMS and FBPA in the matrix.

It was reported that the dielectric properties of the composites with BT nanoparticles strongly depend on their size and relative content in the mixture.[31] The dielectric constants of BT nanoparticles and their composites with polymers are much smaller than that of the bulk BT, and increase with increasing volume fraction of BT particles in the composites. Those measured from the composites with BT particles with a diameter, ranging from 78 nm (calculated dielectric constant of approximately 176) to 442 nm (calculated dielectric constant of approximately 273) in epoxy resins (calculated dielectric constant of approximately 4.5) were reported to be approximately 9−10 at a 14−15 vol % BT loading.[31] These calculated dielectric constants were based on the Lichtenecker equation, which is used to predict the effective dielectric constant of polymer/ceramic composite systems.[32]

Dielectric Properties. The measured ε_1 value of the epoxy composites with the BT powders ranged from approximately 4.5 to 40 as the volume fraction of the BT powders in the composites increased from 0 to 50%. More recently, the dielectric constant of poly(vinylidene-co-hexafluoropropylene) [P(VDF-HFP)] composites with the surface-modified BT particles with an average diameter of 120 nm reached 43 (at 1 kHz) at 50 vol % BT.[15] The increase in the ε_1 of the composite films with the BT nanoparticles originated from the addition of dielectric BT nanoparticles with high permittivity. However, the further addition of BT particles in most BT-filled composites leads to a gradual decrease in the ε_1 value, which is due mainly to the formation of voids and interfacial defects, induced by aggregation or agglomeration between excess BT particles.

The complex dielectric constant ($= \varepsilon_1 + i\varepsilon_2$) of the composite films was measured at frequencies (Hz) of 1×10^3 to 1×10^6 with excitation of 1 V using an LCR meter. A series of thin films of composite materials were prepared by spin-coating viscous solutions of the mixtures of TBT nanoparticles with the ATMS/FBPA hybrid matrix sol on to an ITO substrate, followed by photocuring under UV irradiation ($\lambda = 365$ nm). Parallel plate type capacitors of the composite films were then prepared by evaporating the Ag electrodes on the top of the thin composite film. The average thickness of the spin-coated films was approximately 3 μm, and the volume fraction of the nanoparticles in the mixture was 14%.

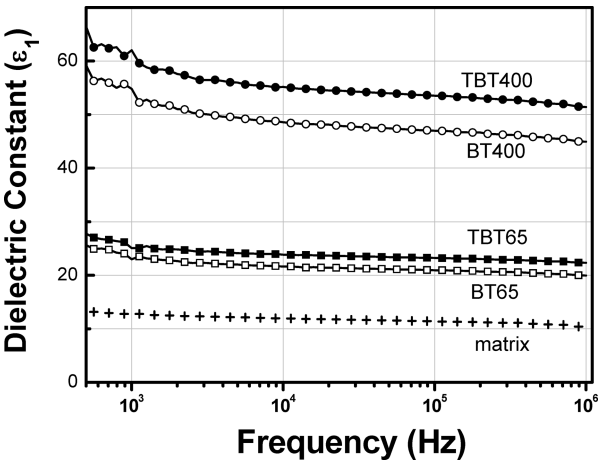

Figure 5. Dielectric constant (ε_1) measured from the host matrix film of ATMS/FBPA (+), and the composite films with BT65 (□), TBT65 (■), BT400 (○), and TBT400 (●).

Figure 5 shows the dielectric constant (ε_1) measured from the host matrix film of ATMS/FBPA, and the composite films with BT65 (□), TBT65 (■), BT400 (○), and TBT400 (●). For each sample, at least several measurements were performed to reach a systematic average. In Figure 5, the measured ε_1 of the host matrix film of ATMS/FBPA was 13 at 1 kHz, which is relatively high compared to those measured from conventional polymeric materials due to the presence of an aromatic bisphenol A unit of FBPA with high electronic polarizability. The measured values of ε_1 of the composite films containing TBT65 and TBT400 (TMSP-coated BT400) were 25 and 62 at 1 kHz, respectively, which are much higher than that measured from the host matrix film. In particular, the measured ε_1 of the composite films with TBT400 was approximately 44% higher than that previously reported for dielectric composites containing BT nanoparticles.[15] The ε_1 value of the TBT composite films could be improved further by the addition of TBT nanoparticles, but <14% TBT or BT nanoparticles was used in this study to maintain the flexibility of the final composite films for potential flexible device applications.

The measured ε_1 from the composite film with the TBT65 and TBT400 nanoparticles was approximately 9 and 13% higher, respectively, than those measured from the composite with the BT nanoparticles (23 and 55 for the composites with BT65 and BT400 nanoparticles, respectively). The large ε_1 value from the composites with TBT particles may be due to a high degree of dispersion of the surface-modified TBT nanoparticles, which had been isolated by very thin passivated layers of ATMS/FBPA matrix, forming many nanoscale capacitors, leading to composite films with a very large dielectric constant.[33] As shown in Figure 4, a part of the BT65 nanoparticles forms agglomerates in the matrix, whereas most TBT particles were well dispersed and coated completely with the matrix of ATMS/FBPA. The better dispersion of TBT

(31) Cho, S.-D.; Lee, S.-Y.; Hyun, J.-G.; Paik, K.-W. *J. Mater. Sci. Mater. Electron.* **2005**, *16*, 77–84.
(32) Mazur, K. *Plast. Eng.* **1995**, *28*, 539–610.
(33) He, F.; Lau, S.; Chan, H. L.; Fan, J. *Adv. Mater.* **2009**, *21*, 710–715.

nanoparticles in the matrix was mainly due to the presence of an organic layer of TMSP attached to the BT nanoparticles, which causes steric hindrance between the TBT particles and prevents aggregation of the dispersed phase both in the mixture sol and in the final composites. The silane units of TMSP were also reacted with those of ATMS in the ATMS/FBPA matrix during the sol−gel reaction, which produces a networklike interface with the hybrid matrix. Moreover, the porosity and interfacial defects could be prevented by a sol−gel reaction at the interfaces.

The large increase in ε_1 value from the TBT and BT composite films even at low particle loadings was due partly to the polar matrix of the ATMS and FBPA units, which improves the dispersibility of BT nanoparticles in the matrix. Under these circumstances, the dielectric TBT or BT nanoparticles were surrounded by the polar matrix of the ATMS and FBPA units, which causes a large increase in the dielectric constant of the final films. The halogenated, aromatic bisphenol A units of FBPA exhibited high electronic polarizability in an external electric field, which might induce orientational and interfacial polarization, particularly at the interfaces with dielectric particles based on the percolation theory in the case of a high degree of dispersion of dielectric BT nanoparticles.[34]

Figure 6 shows the dielectric loss tan δ ($= \varepsilon_2/\varepsilon_1$) of the composite films with BT and TBT nanoparticles as a function of the frequency. The dielectric loss decreased with increasing frequency from 1 kHz to ~10 kHz, mainly due to the space charge effect, but thereafter became almost constant within a narrow range of 0.01−0.02. At a high frequency of 1 MHz, all measured loss values were quite low ($\leq$0.01). Such low dielectric loss was obtained by the presence of a dense, nanoscale TMSP-coated or passivated layer onto the particles, which forms an insulating boundary outside of the dielectric cores to restrict charge transfer between the dielectric nanoparticles. In Figure 6, the loss values of the composites containing the TBT65 and TBT400 nanoparticles were always lower than those containing the corresponding BT65 and BT400 nanoparticles, respectively, indicating that the TMSP passivated layers of nanoparticles play a key role in minimizing the mobility of charge carriers, thereby ensuring composites with dielectric nanoparticles with low dissipation factors. The dielectric loss of the composites of the surface-modified BT with the ATMS/FBPA host matrix was <0.01 at 1 MHz because of the improved dispersibility and interfacial adhesion of BT particles in the ATMS/FBPA host matrix. The surface modification by phosphonic acid improves the adhesion of BT nanoparticles with the matrix and decreases the porosity or interfacial defects, leading to a decrease in dielectric loss of the composites.

The breakdown strength, which is defined as the maximum electric field needed to cause dielectric breakdown through the material, was accompanied by a sharp increase in current density. Figure 7 shows the breakdown strength

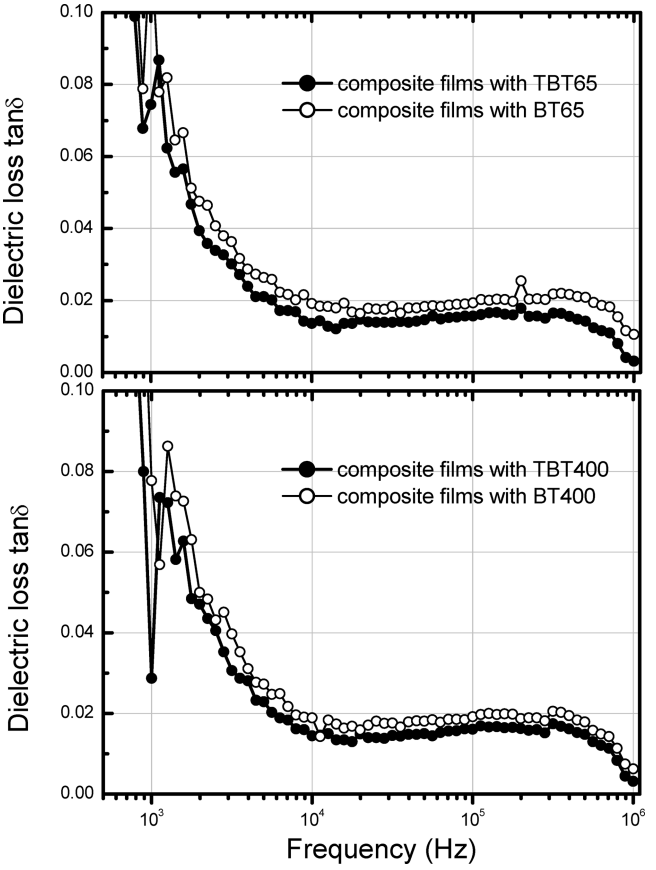

Figure 6. Dielectric loss tan δ ($= \varepsilon_2/\varepsilon_1$) for the composite films with BT65 (○) and TBT65 (●) nanoparticles (top); and BT400 (○) and TBT400 (●) nanoparticles (bottom) as a function of frequency.

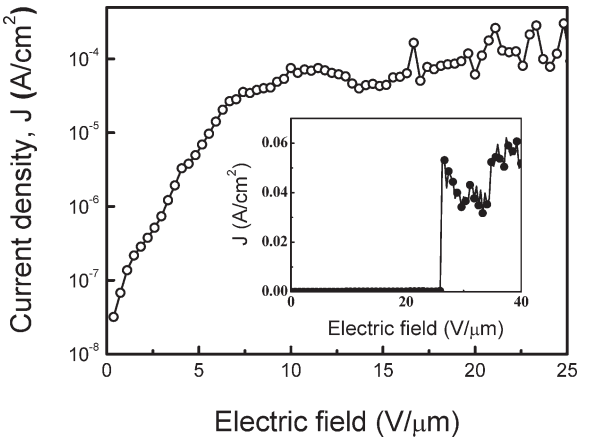

Figure 7. Breakdown strength of the composites with the TBT65 particles.

of the composites with the TBT65 particles. The breakdown field was 263 V μm^{-1}, which was larger than that for conventional polymeric materials. As demonstrated in Figure 7, a high breakdown strength and low leakage current of the composite films were obtained by effective surface modification and a high degree of dispersion of the TBT65 particles within the matrix. As shown in Figure 1, the BT particles were coated completely with the thick TMSP organic layer that provides reactive sites for the silane units of ATMS in the matrix, and reduces

(34) Miyamoto, T.; Shibayama, K. *J. Appl. Phys.* **1973**, *44*, 5372–5376.

the leakage currents and sources of runaway conduction that can lead to dielectric breakdown.

Conclusions

A series of novel high-κ thin composite films were successfully synthesized using nonhydrolytic sol−gel processing. The organic−inorganic hybrid material with high electronic polarizability was prepared and used as the matrix material to form a covalently bonded interface with the organically modified BT nanoparticles. A high degree of dispersion of the dielectric BT nanoparticles in the matrix with high electronic polarizability significantly improves the dielectric properties of the final composite films such as high dielectric constant and excellent breakdown strength. In addition, these final composite films display the excellent mechanical integrity, as evidenced by its flexibility, toughness, and adhesion, which can be tailored to meet the needs of specific electronic applications.

Acknowledgment. This work was supported by the National Research Foundation of Korea Grant funded by the Korean Government (MEST) (NRF-2009-C1AAA001-2009-0093204).